# Tribological Behavior of Inconel 718 Nickel-Based Super Alloy Doped with Graphene Nanoplatelets*

**Khotso Khoele[1, 3**], Onoyivwe Monday Ama [2, 3], David Disai[4], David Jacobus Delport[1] and Suprakas Sinha Ray[3]**

*[1]Tshwane University of Technology, Department of Chemical, Metallurgical and Materials Engineering, Pretoria, South-Africa*
*[2]Department of Chemical Science, University of Johannesburg, Doornfontein, Johannesburg, South Africa*
*[3]DST-CSIR National Center for Nanostructured Materials Council for Scientific and Industrial Research, Pretoria, South Africa*
*[4]Tshwane University of Technology, Department of Mechanical and Industrial Engineering*
**Corresponding author: khotsokhoele@gmail.com

Received 21/09/2021; accepted 15/12/2021
https://doi.org/10.4152/pea.2023410102

**Abstract**
In continuation of our previously published work entitled *Mechanical and Corrosion Behavior of Inconel 718 Nickel-Based Super Alloy Doped with Graphene Nanoplatelets*, the present study investigated the tribological performance of modified IN 718 doped with GrNs. Friction and wear properties were analised using an advance universal tribometer, while surface mophologies were studied by SEM. The modified SA tribological properties validation was done in relative comparison to those of pure IN 718**.** Mechanical properties with higher η, younger modulus values, better morphologies, higher AWI, lower SWR and μ values were noted on the modified IN 718. Nonetheless, an increase in the load proved to affect the tribological oxide layer properties of both pure and modified IN 718.

***Keywords:*** pure and modified IN 718, GrNs, frictional wear, tribology and SEM.

## Introduction

IN 718 Ni-based SA is known to possess higher tensile strength, excellent creep resistance, low-cycle fatigue strength, good formability and weldability [1-10]. Hence, it is often chosen as a good alloy, to be used for high speed machinery shafts. However, it has been found that IN 718 is pronouncely affected by frictional wear during its application. In most cases, this SA serious drawbacks during applications are due to its difficulties during machining. In fact, IN 718 is widely known to have poor thermal conductivity, work hardening high rate, high η and chemical affinity towards cutting tool materials [11-15]. All these inherent properties not only are

*The abbreviations and symbols definitions lists are in pages 24-25.

problematic to the machining processes, but also render this SA susceptible to inferior mechanical properties, corrosion and frictional wear during its applications.
In an endeavour to improve IN 718 corrosion, surface and mechanical properties, at elevated temperatures [16], we doped it with GrNs. From the engaged methods and analyses, higher η values were obtained. Furthermore, less reduction of the young modulus values occurred during high temperature oxidation. PDP curves also showed more electropositive $E_{corr}$ and lower $I_{corr}$ values for the modified IN 718. Most notably, GrNs, η and EIS measurements showed a strong oxide layer that is more corrosion mitigative. Likewise, morphologies showed no localized corrosion under all conditions. All those features proved that IN 718 doping by GrNs played a significant role in improving its corrosion resistance, mechanical and surface properties [17]. Nonetheless, frictional wear analyses were not conducted.
Hence, the present study investigated and reported on the modified IN 718 tribological performance, which was fabricated by selective laser melting. Investigations were made on wear and frictional properties, under room temperature. Surface morphologies were also incorporated into reference to the tribological impact. All comparisons were made relative to the IN 718 standard material.

## Experimental

### *Materials*

Both pure and modified IN 718 were supplied in a dimensional size of 15 × 15 × 5 mm.

### *Hardness and modulus of elasticity measurements*

Mechanical properties were clarified from η and young modulus analyses. The η depths were measured using ASTM E384-05 criterion that is described elsewhere [18]. Young modulus tests on both bare and coated foils were carried out following EN 10002-1 measurement guide lines, and they were performed by an Instron 3384 testing machine.

### *Surface characterizations*

SEM was used to examine the surface morphologies, while XRD was used to determine phases of the oxides phases which that were formed during the tribological tests.

### *Tribological set-up and measurements*

Friction and wear properties of bare and nano-coated foils were studied by a RTEC2441 (s/n :, USA) universal tribometer. The measurements were carried out at room temperature. The tests were run under dry lubrication conditions that are explained further ahead. A steel ball was used as the counterpart material against both standard and modified materials. The diameter size of the steel ball was 1.50 mm, and the acquisition rate was 3.14 Hz, with an equivalent stroke length of 6 mm. The measurements were intended to incorporate friction and wear properties from both pure and modified IN 718.

### *SWRs and AWIs*

AWIs and SWRs calculations were carried out from the equations 1 and 2 below.

$$AWI = \frac{\text{MB}\cdot\text{DC WRB}}{\text{MC}\cdot\text{ DB WRC}} \quad (1)\ [19]$$

where: $M_B$ and $M_C$ are the mass loss from the bare and coated foils, respectively; $D_C$ and $D_B$ are the density of the coated and bare foils, respectively; and $WR_B$ and $WR_C$ are the total number of wheel revolutions during the tests on the bare and coated foils, respectively.

$$SWR = \frac{\text{V}}{\text{F}\cdot\text{L}} = \frac{\text{m}}{\text{F}\cdot\text{L}\cdot\text{p}}\left[\frac{mm^3}{N\cdot m}\right] \quad (2)\ [19]$$

where: V is the velocity (m/s); F is the force (10 N); L is the total sliding distance; and m and p are the engaged material mass loss and density, respectively.

## Results and discussion

### *Hardness and modulus of elasticity measurements*

Fig. 1 shows the mechanical properties of both pure and modified IN 718. As it can be seen in Fig. 1, pure IN 718 has lower η and younger modulus values than those of the modified one. Confirming the mechanical properties criterion that generally recognizes improvement of materials possessing higher η and modulus elasticity values [20-25], the incorporated nanoplatelets GrNs provided better tribological properties.

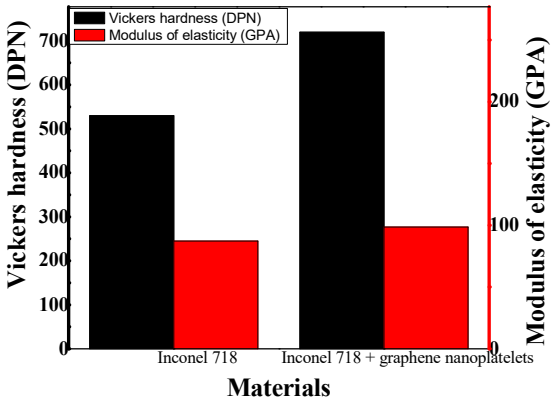


**Figure. 1** Elasticity modulus and η of both pure and modified IN 718.

### *Tribology measurements (wear and friction)*

*SWR and AWI rate*

Overall wear analyses on both pure and modified IN 718 are displayed in Fig. 2 and 3. As it can be seen in Fig. 2, AWI is much higher for the modified IN 718. On the other hand, pure IN 718 had higher SWR than that of the modified one, as it can be

seen in Fig. 3, which suggests better tribological properties of the modified IN 718 [26-30].

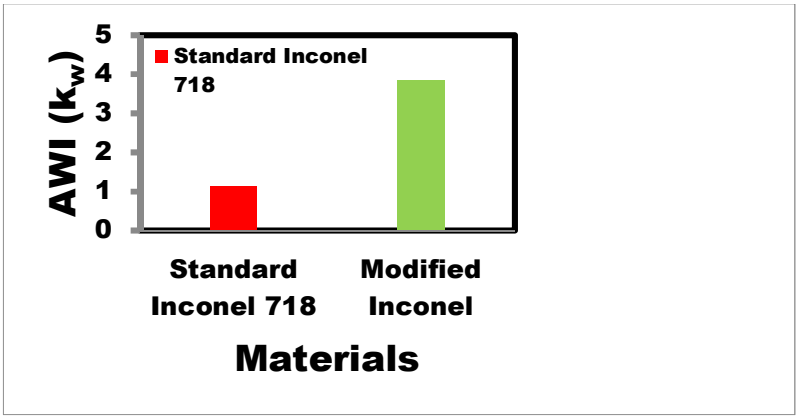


**Figure. 2** AWI for both pure and modified IN 718.

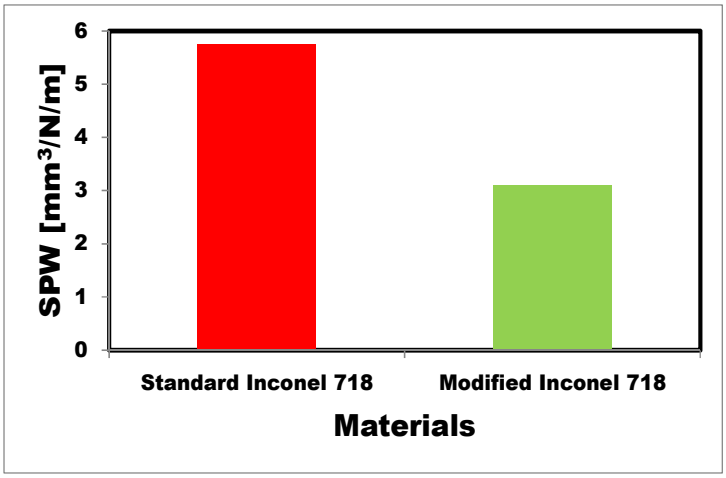


**Figure. 3.** SWR for both pure and modified IN 718.

***Analyses of μ***

The μ analyses on both pure and modified IN 718, in a progression of time under no loads and several loads, are shown in Figs. 4 and 5. As it can be seen in Fig. 4, an increase in the load rapidly affected the oxide layer and μ on the pure IN 718 surface. Furthermore, an occurrence of a running-in period is swhon n Fig. 4 (i and iii), which could be due to an interlock of asperities between IN 718 and the steel ball from the tribometer [31]. In Fig. 4 (ii), it can be seen that μ starts by decreasing, and this phenomenon is called transient period, during which IN 718 was suspended in a space where it was smoothed before its oxide layer was transferred to the steel ball. As time went by, minor fluctuations occurred on the oxide layer formed under no load conditions. However, as the load was increased, major fluctuations occurred on pure IN 718.

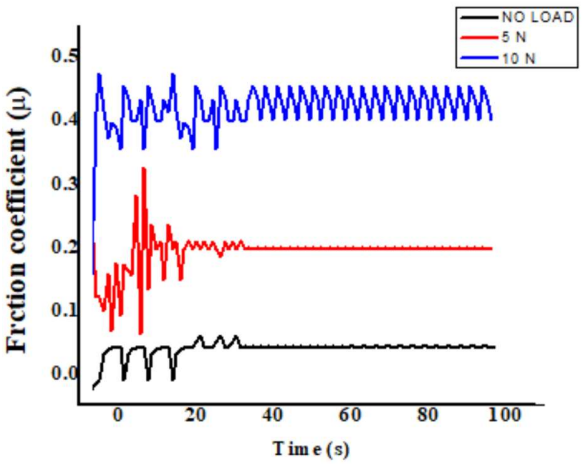


**Figure. 4.** μ of pure IN 718 under no load and several low loads (5 to 10 N), in a progression of time.

The running-in period was also observed on modified IN 718, as it can be seen from Fig. 5. Nevertheless, μ was lower under all conditions. An improvement observed on the modified IN 718 was due to Gr oxidation, which gave a better structural strength to the SA, thus improving its load carrying capacity [32, 33]. An increase in the load was also found to have caused fluctuations on the steady-state condition of the oxide layer, during the modified IN 718 tribological measurement. There are normally two factors that could lead to aggressive tribological conditions, as the load increases: a friction-induced thermal effect during sliding, under high loads [34]; and an increased contact between the rubbed surfaces, which was excerbated by the higher load [35, 36]. Therefore, it was noted the cushion formation of an oxide layer that acted as buffer (immunity), detering IN 718 surface wear.

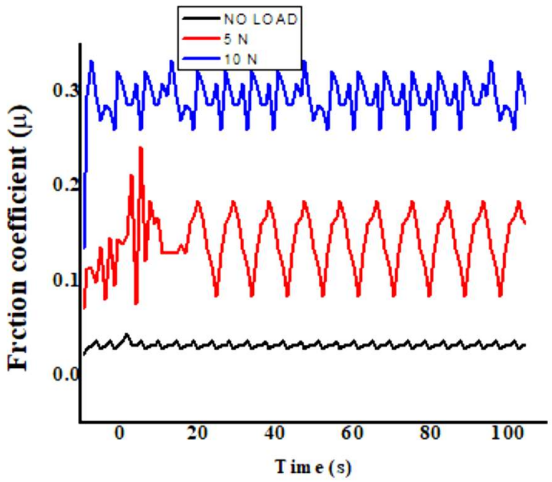


**Figure. 5.** μ of modified IN 718 under no load and several low loads (5 to 10 N), in a progression of time.

***SEM analyses***

SEM micrographs for the engaged substrates, before tribological measurements, are shown in Fig. 6, while the ones captured after tribological measurements are shown in Figs. 7 and 8.

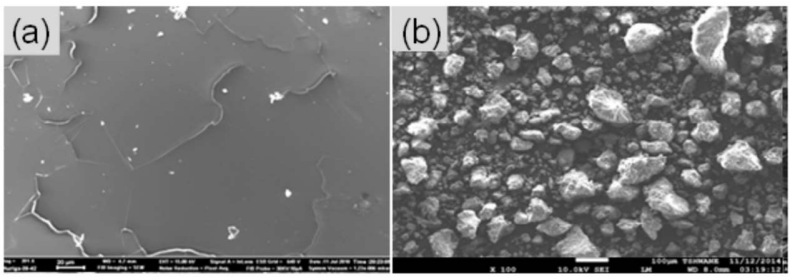


**Figure. 6.** Surface morphologies on IN 718: **(a)** bare; **(b)** and modified, before tribological measurements [18].

Shallow inclusions and voids, under no load conditions, on pure IN 718, can be seen in Fig 7 (a). As the load was increased to 5 N, ploughs, voids and pores were discovered on pure IN 718 surface, as it can be seen in Fig. 7 (b). At the load of 10 N, tracks were discovered on its surface, which can be seen in Fig. 7 (c).

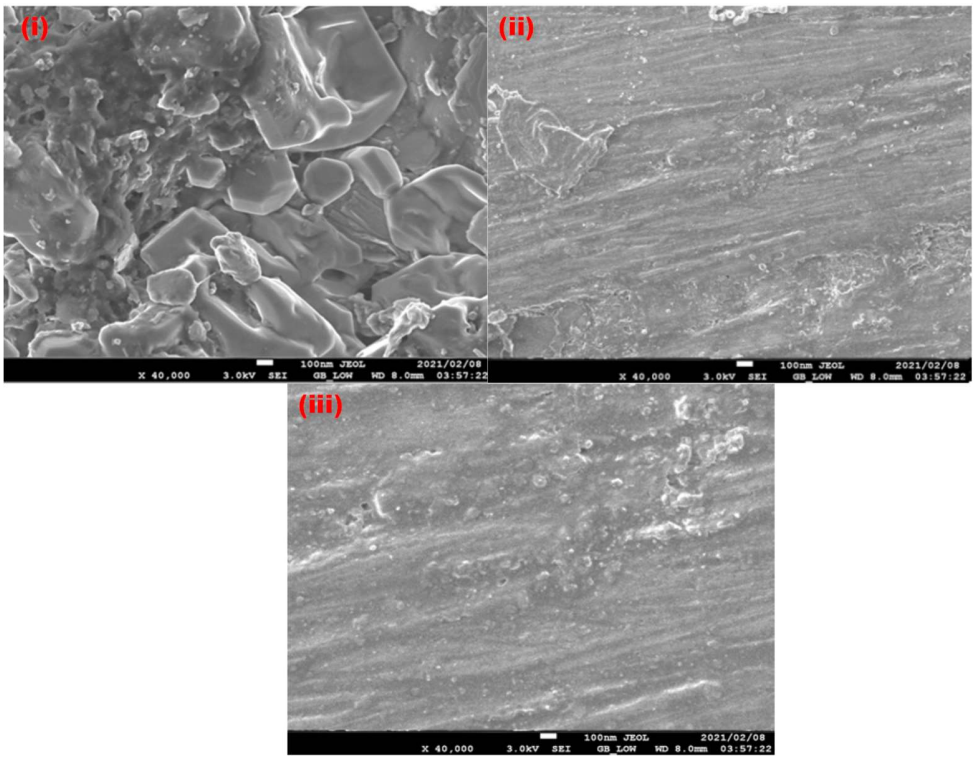


**Figure 7.** Surface morphologies on: **(i)** pure IN 718 under no load; **(ii)** 5 N applied load; and **(iii)** 10 N applied load, in a progression of time.

Contrarily, micrographs of a smooth oxide layer can be noticed on modified IN 718 surface, which are shown in Fig. 8 (a). At an applied load of 5 N, shallow fine grooves were noticed. The corresponding scan is shown in Fig. 8 (b). With the increase in load to 10 N, shallow ploughs were found on its surface, as it can be seen in Fig. 8 (c). SEM analyses, herein, corroborate the earlier results on SWR and μ coefficient. This observation, therefore, strongly suggests that GrNs incorporation into the IN 718 provided improved mechanical properties and a tribological oxide layer which lowered the frictional wear.

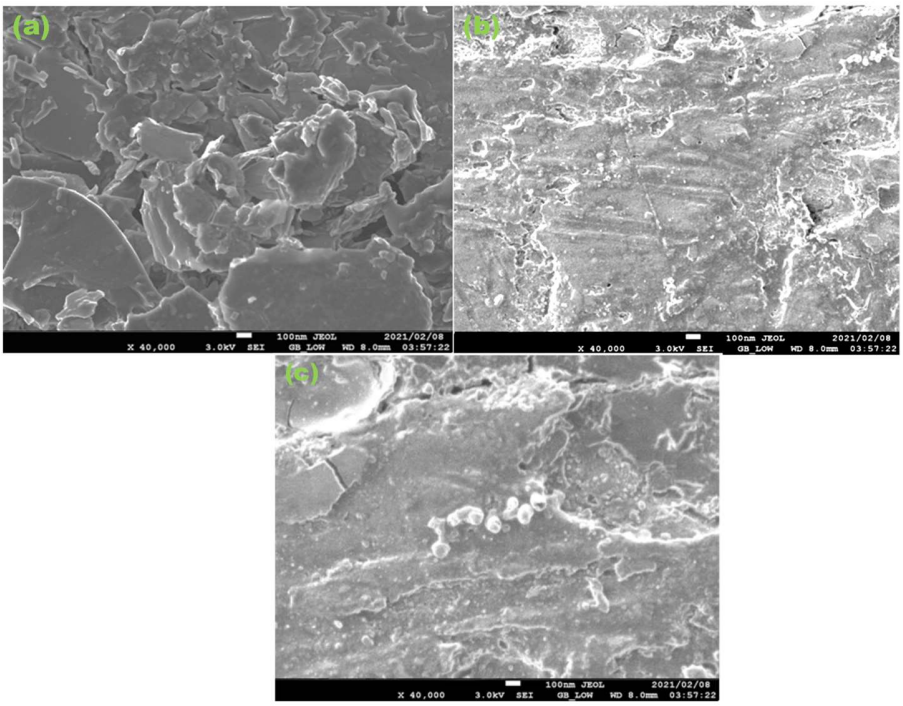


**Figure. 8.** Surface morphologies on modified IN 718: **(a)** under no load; **(b)** 5 N applied load; and **(c)** 10 N applied load, in a progression of time.

## Conclusions

The tribological characterization of both pure and modified IN 718 has throughly been investigated in this study. The following conclusions were drawn up from the main findings:

- Modified IN 718 possessed higher η and younger modulus values.
- Pure IN 718 had relatively lower AWIs. Contrarily, higher AWIs and lower SWRs were discovered for the modified IN 718.
- Lower μ values were noted, under all the conditions, on the modified IN 718. However, an increase in the load proved to affect the tribological oxide layer of both pure and modified IN 718.
- Shallow inclusions and voids were not noted in the pure IN 718 morphologies, under no load condition, while voids and pores were discovered for an

increased load of 5 N on the pure SA. Moreover, micrographs composed of wear tracks were noted at 10 N applied load on pure IN 718.

- Contrarily, micrographs showed a smooth oxide layer formed on the modified IN 718 surface, under no load condition. With an increase in the loads to 5 and 10 N, shallow fine grooves and shallow ploughs, respectively, were noticed on the modified SA.
- Generally, GrNs incorporation into IN 718 provided improved mechanical properties and a tribological oxide layer, which lowered frictional wear.

**Acknowledgement**
We would like to thank DAAD/NRF for funding this study, and Powerkote (PTY) LTD for availing the foils for the research.

**Declaration**
This study was funded by the German Research Exchange (DAAD/NRR in Country), and the materials used were supplied by Powerkote. There are no conflicts of interest towards the submission of this manuscript. However, some information remains as intellectual property (IP) from Powerkote. Hence, the coating materials have not been disclosed. Data and software used in the application of nanocomposites on the foils remains confidential. All parties involved in this work are consenting and aware of the publication of this work. Most importantly, all ethics were mandatorily obeyed.

**Authors' contributions**
**Khotso Khoele**: conceived and designed the analysis; collected the data; performed every analysis; inserted the data or analysis tools; wrote the paper. **Onoyivwe Monday Ama**: contributed with the analysis of the results; edited the work on data and inserted analysis tools. **David Disai**: edited the work at certain parts. **David Jacobus Delport**: designed the analysis; contributed on the paper writing. **Suprakas Sinha Ray**: made overall editing of the work; provisioned equipment for the characterization of the samples.

**Abbreviations**
**AWI**: abrasive wear index
**$E_{corr}$**: corrosion potential
**EIS**: electrochemical impedance spectroscopy
**GrNs**: graphene nanoplatelets
**$I_{corr}$**: corrosion current density
**IN 718**: Inconel 718
**IN 718 + GrNs**: modified IN 718
**Ni**: nickel
**PDP**: potentiodynamic polarization
**SA**: super alloy
**SEM**: scanning electron microscopy

**SWR**: specific wear rate
**XRD**:X-ray diffraction

**Symbols definitions:**
**μ**: friction coefficient
**η**: hardness

## References

1. Mortezaie A, Shamanian M. An assessment of microstructure, mechanical properties and corrosion resistance of dissimilar welds between Inconel 718 and 310S austenitic stainless steel. Int J Press Vessels Pip. 2014;116:37-46. https://doi.org/10.1016/j.ijpvp.2014.01.002
2. Tan L, Ren X, Sridharan K et al. Corrosion behavior of Ni-base alloys for advanced high temperature water-cooled nuclear plants. Corros Sci. 2008;50(11):3056-3062. https://doi.org/10.1016/j.corsci.2008.08.024
3. Mei Y, Liu Y, Liu C et al. Effect of base metal and welding speed on fusion zone microstructure and HAZ hot-cracking of electron-beam welded Inconel 718. Mater Des. 2008;89:964-977. https://doi.org/10.1016/j.matdes.2015.10.082
4. Ramkumar T, Selvakumar M, Narayanasamy P et al. Studies on the structural property, mechanical relationships and corrosion behaviour of Inconel 718 and SS 316L dissimilar joints by TIG welding without using activated flux. J Manuf Process. 2017;30: 290-298. https://doi.org/10.1016/j.jmapro.2017.09.028
5. Kurzynowski T, Smolina I, Kobiela K et al. Wear and corrosion behaviour of Inconel 718 laser surface alloyed with rhenium. Mater Des. 2017;132:349-359. https://doi.org/10.1016/j.matdes.2017.07.024
6. Chen T, Nutter J, Bai J et al. Corrosion fatigue crack growth behavior of oil-grade nickel-base alloy 718. Part 2: effect of aging treatment. Corros Sci. 2015;98:280-290. https://doi.org/10.1016/j.corsci.2015.05.033
7. Chen T, Nutter J, Hawk J et al. Corrosion fatigue crack growth behavior of oil-grade nickel-base alloy 718. Part 1: effect of corrosive environment. Corros Sci. 2014;89:146-153. https://doi.org/10.1016/j.corsci.2014.08.022
8. Tucho WM, Cuvillier P, Sjolyst-Kverneland A et al. Microstructure and hardness studies of Inconel 718 manufactured by selective laser melting before and after solution heat treatment. Mater Sci Eng A. 2017;689:220-232. https://doi.org/10.1016/j.msea.2017.02.062
9. Pradhan D, Mahobia GS, Chattopadhyay K et al. Severe hot corrosion of the super alloy IN 718 in mixed salts of $Na_2SO_4$ and $V2O_5$ at 700 C°. J Mater Eng Perform. 2018;27(8):4235-4243. https://doi.org/10.1007/s11665-018-3501-9
10. Sun SH, Koizumi Y, Saito T et al. Electron beam additive manufacturing of Inconel 718 alloy rods: Impact of build direction on microstructure and high temperature tensile properties. Addit Manuf. 2018;23:457-470. https://doi.org/10.1016/j.addma.2018.08.017
11. Sivalingam V, Zan Z, Sun J et al. Wear behaviour of whisker-reinforced ceramic tools in the turning of Inconel 718 assisted by an atomized spray of solid lubricants. Tribolog Int. 2020;148:106235. https://doi.org/10.1016/j.triboint.2020.106235

12. Marques A, Suarez MP, Sales WF et al. Turning of Inconel 718 with whisker-reinforced ceramic tools applying vegetable-based cutting fluid mixed with solid lubricants by MQL. J Mat Proc Eng Tech. 2019;266:530-543. https://doi.org/10.1016/j.jmatprotec.2018.11.032
13. Hosseini E, Popovich VA. A review of mechanical properties of additively manufactured Inconel 718. Addit Manufact. 2019;30:100877. https://doi.org/10.1016/j.addma.2019.100877
14. Kumar SA, Raman SGS, Narayanan TS et al. Fretting wear behavior of surface mechanical attrition treated alloy 718. Surf Coat Technol. 2012;206:4425-4432. https://doi.org/10.1016/j.surfcoat.2012.04.085
15. Zou B, Chen M, Huang C et al. Study on surface damages caused by turning $NiCr_{20}TiAl$ nickel-based alloy. J Mat Proc Technol. 2009;5802-5809. https://doi.org/10.1016/j.jmatprotec.2009.06.017
16. Radil K, Zeszotek M. An experimental investigation into the temperature profile of a compliant foil air bearing. Tribol Trans. 2004;47(4):470-479. https://doi.org/10.1080/05698190490501995
17. Khoele K, Delport DJ. Mechanical and Corrosion Behavior of Inconel 718 Nickel-Based Super Alloy Doped with Graphene Nanoplatelets. J Fail Analyt Prev. 2019;19(5):1493-1497. https://doi.org/10.1007/s11668-019-00754-3
18. Jia Q, Gu D. Selective laser melting additive manufacturing of Inconel 718 super alloy parts: Densification, microstructure and properties. J Alloy Comp. 2014;585:713-721. https://doi.org/10.1016/j.jallcom.2013.09.171
19. Kurzynowski T, Smolina I, Kobiela K et al. Wear and corrosion behaviour of Inconel 718 laser surface alloyed with rhenium. Mat Des. 2017;132:349-359. https://doi.org/10.1016/j.matdes.2017.07.024
20. Rashad M, Pan F, Tang A et al. Improved strength and ductility of magnesium with addition of aluminum and graphene nanoplatelets using semi powder metallurgy method. J Ind Eng Chem. 2015;23: 243-250. https://doi.org/10.1016/j.jiec.2014.08.024
21. Nieto A, Lahiri D, Agarwal A. Synthesis and properties of bulk graphene nanoplatelets consolidated by spark plasma sintering. Carbon. 2012;50(11):4068-4077. https://doi.org/10.1016/j.carbon.2012.04.054
22. Chatterjee S, Nafezarefi F, Tai NH et al. Size and synergy effects of nanofiller hybrids including graphene nanoplatelets and carbon nanotubes in mechanical properties of epoxy composites. Carbon. 2021;50(15):5380-5386. https://doi.org/10.1016/j.carbon.2012.07.021
23. Geng Y, Wang SJ, Kim JK. Preparation of graphite nanoplatelets and graphene sheets. J Coll Interf Sci. 2009;336(2):592-598. https://doi.org/10.1016/j.jcis.2009.04.005
24. Rashad M, Pan F, Tang A et al. Synergetic effect of graphene nanoplatelets (GNPs) and multi-walled carbon nanotube (MW-CNTs) on mechanical properties of pure magnesium. J Alloy Comp. 2014;603:111-118. https://doi.org/10.1016/j.jallcom.2014.03.038
25. Chen H, Ba Z, Qiao D, Feng D et al. Study on the tribological properties of graphene oxide composite films by self-assembly. Tribol Int. 2020;151:106533. https://doi.org/10.1016/j.triboint.2020.106533
26. Wang Y, Ji H, Li L et al. Trilayered film with excellent tribological performance: a combination of graphene oxide and perfluoropolyethers. Tribol Lett. 2015;60(3):41. https://doi.org/10.1007/s11249-015-0618-y

27. Bashandeh K, Lan P, Meyer JL et al. Tribological performance of graphene and PTFE solid lubricants for polymer coatings at elevated temperatures. Tribol Lett. 2019;67(3):99.
28. Dass K, Chauhan SR, Gaur B. Study on the effects of nano-aluminum-oxide particulates on mechanical and tribological characteristics of chopped carbon fiber reinforced epoxy composites. Proc Inst Mech Eng Part J Mater Des Appl. 2017;231:403-22. https://doi.org/10.1177/1464420715598798
29. Che Y, Sun Z, Zhan R et al. Effects of graphene oxide sheets- zirconia spheres nanohybrids on mechanical, thermal and tribological performances of epoxy composites. Ceram Int. 2018;44:18067-77. https://doi.org/10.1016/j.ceramint.2018.07.010
30. Ibrahim AMM, Mohamed AFA, Fathelbab AM et al. Enhancing the tribological performance of epoxy composites utilizing carbon nano fibers additives for journal bearings. Mater Res Express. 2018;6:035307. https://doi.org/10.1088/2053-1591/aadcdc
31. Hou G, An Y, Zhao X et al. Improving interfacial, mechanical and tribological properties of alumina coatings on Al alloy by plasma arc heat-treatment of substrate. Appl Surf Sci. 2017;411:53-66. https://doi.org/10.1016/j.apsusc.2017.03.170
32. Sharma SK, Biswas K, Majumdar JD. Wear behaviour of electron beam surface melted Inconel 718. Procedia Manufacturing. 2019;35:866-87. https://doi.org/10.1016/j.promfg.2019.06.033
33. Hou G, An Y, Zhao X et al. Improving interfacial, mechanical and tribological properties of alumina coatings on Al alloy by plasma arc heat-treatment of substrate. Appl Surf Sci. 2017;411:53-66. https://doi.org/10.1016/j.apsusc.2017.03.170
34. Kandanur SS, Rafiee MA, Yavari F et al. Suppression of wear in graphene polymer composites. Carbon. 2012;50(9):3178-83. https://doi.org/10.1016/j.carbon.2011.10.038
35. Ou J, Wang Y, Wang J et al. Self-assembly of octadecyltrichlorosilane on graphene oxide and the tribological performances of the resultant film. J Phys Chem C. 2012;115(20):10080-6. https://doi.org/10.1021/jp200597k
36. Min C, Liu D, Qian J et al. High mechanical and tribological performance polyimide nanocomposites using amine-functionalized graphene nanosheets. Tribol Int. 2019;131:1-10. https://doi.org/10.1016/j.triboint.2018.10.013